



## UvA-DARE (Digital Academic Repository)

### What Determines the Breakup Length of a Jet

Kooij, Stefan; Jordan, Daniel T.A.; Van Rijn, Cees J.M.; Ribe, Neil M.; Bonn, Daniel

**DOI**

[10.1103/jf6w-l5sy](https://doi.org/10.1103/jf6w-l5sy)

**Publication date**

2025

**Document Version**

Final published version

**Published in**

Physical Review Letters

**License**

CC BY

[Link to publication](#)

**Citation for published version (APA):**

Kooij, S., Jordan, D. T. A., Van Rijn, C. J. M., Ribe, N. M., & Bonn, D. (2025). What Determines the Breakup Length of a Jet. *Physical Review Letters*, 135(21), Article 214001. <https://doi.org/10.1103/jf6w-l5sy>

**General rights**


It is not permitted to download or to forward/distribute the text or part of it without the consent of the author(s) and/or copyright holder(s), other than for strictly personal, individual use, unless the work is under an open content license (like Creative Commons).

**Disclaimer/Complaints regulations**

If you believe that digital publication of certain material infringes any of your rights or (privacy) interests, please let the Library know, stating your reasons. In case of a legitimate complaint, the Library will make the material inaccessible and/or remove it from the website. Please Ask the Library: <https://uba.uva.nl/en/contact>, or a letter to: Library of the University of Amsterdam, Secretariat, P.O. Box 19185, 1000 GD Amsterdam, The Netherlands. You will be contacted as soon as possible.

## What Determines the Breakup Length of a Jet?

Stefan Kooij,<sup>1</sup> Daniel T. A. Jordan<sup>1,2</sup>, Cees J. M. van Rijn,<sup>1</sup> Neil M. Ribe<sup>3</sup>, and Daniel Bonn<sup>1</sup>  
<sup>1</sup>*Van der Waals-Zeeman Institute, University of Amsterdam, Science Park 904, Amsterdam, The Netherlands*  
<sup>2</sup>*Institute of Physics, University of Amsterdam, Science Park 904, 1098 XH Amsterdam, The Netherlands*  
<sup>3</sup>*Laboratoire FAST, Université Paris-Saclay, CNRS, 91405 Orsay, France*

 (Received 20 December 2024; revised 28 May 2025; accepted 2 October 2025; published 17 November 2025)

The breakup of a capillary jet into drops is believed to be governed by initial disturbances on the surface of the jet that grow exponentially. The disturbances are often assumed to be due to external sources of noise, to turbulence, or to imperfections of the nozzle. Here we demonstrate that the initial disturbances observed across a wide range of conditions are quantitatively consistent with thermal capillary waves, where the initiating disturbances must be of the order of an angstrom, suggesting that thermal noise can act as a primary driver of jet breakup under typical experimental conditions. Our experiments with a wide range of nozzles show no significant variation in breakup length linked to nozzle type, shape, or inner roughness. By systematically varying the jet diameter and velocity and the fluid properties, we validate our thermal disturbance model over 4 orders of magnitude in jet length, and 7 orders of magnitude when previous molecular dynamics simulations and stochastic hydrodynamics calculations of nanojets are included.

DOI: [10.1103/jf6w-15sy](https://doi.org/10.1103/jf6w-15sy)

The breakup of laminar liquid jets is of fundamental importance in both natural and industrial processes, with applications ranging from inkjet printing and DNA sampling to food processing and drug delivery [1–6]. Lord Rayleigh showed that breakup of an axisymmetric jet is due to small initial disturbances that grow exponentially [6–12]. The initial perturbations are often assumed to be due to environmental sources of noise such as vibrations, or to imperfections of the liquid flow through the orifice or capillary. Savart noticed in 1833 that the intact length of a jet may be increased “by suitable insulation of the reservoir from tremors,” but added that “it does not appear to be possible to carry the prolongation very far” [7]. Later studies suggest that there is always some level of residual disturbances that can lead to breakup, the origin of which remains unclear [9]. A recent suggestion is that the disturbances may be due to previous breakup events themselves, leading to a self-sustaining “natural” breakup length for the jet [13]. Evidently, the breakup of liquid jets remains an outstanding scientific problem nearly 200 years after Savart’s pioneering work.

Because natural jet breakup is irregular, breakup lengths and droplet sizes vary significantly (Fig. 1), underscoring the need to understand the mechanisms that govern jet breakup. Here we investigate the origin of the initial

disturbances and find, contrary to prevailing assumptions, that they are not due to nozzle imperfections, environmental noise, or noise from the breakup itself. Instead, we propose that the disturbances are due to thermal capillary waves, i.e., thermal fluctuations, recently shown in simulations to influence breakup patterns [14,15]. Using high-speed imaging, we track the growth of visible disturbances on the jet surface. We estimate the magnitude of the initial perturbations to be on the order of 1 Å, which is the typical amplitude of thermal capillary waves or thermal surface roughness. Combining our experimental results with earlier molecular dynamics (MD) simulations and a stochastic hydrodynamics treatment where thermal noise is included [16], we find that a simple model of breakup triggered by thermally driven disturbances consistently predicts jet lengths across more than 7 orders of magnitude, from nanoscale to macroscopic jets.

Our experimental setup is shown in Fig. 1(c). We used five nozzle geometries (Fig. 2), with hole diameters from 4 mm down to 4 μm. Viscosity  $\mu$  was varied from 1 to 15 mPa s by using water-glycerol solutions. Surface tension  $\gamma$  was varied by using both water-ethanol solutions (22–72 mN m<sup>-1</sup>) and the eutectic liquid galinstan (718 mN m<sup>-1</sup>). Density  $\rho$  was varied using the aforementioned liquid mixtures as well as galinstan (density 6.44 g cm<sup>-3</sup>). The galinstan jet experiment was performed in vacuum to prevent the formation of an oxide layer. To pressurize the liquid we employed several techniques such as an high-performance liquid chromatography (HPLC) pump (Waters 515), a pressure tank, a handheld syringe, or simply the tap water installation. Flow rates were determined using image analysis or pressure sensor data, or by collecting and weighing the ejected liquid

---

*Published by the American Physical Society under the terms of the Creative Commons Attribution 4.0 International license. Further distribution of this work must maintain attribution to the author(s) and the published article’s title, journal citation, and DOI.*

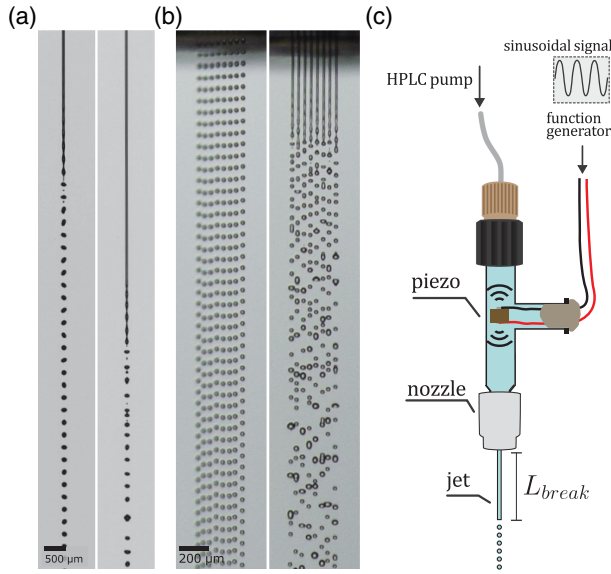


FIG. 1. Perturbed versus unperturbed water jets. (a) Single 64  $\mu\text{m}$  diameter jet at 2 bar, without perturbations (right) and perturbed at  $f = 28.2$  kHz (left). (b) Eight 16  $\mu\text{m}$  diameter jets, unperturbed (right) and perturbed (left). (c) Jets are perturbed using a submerged piezoelectric transducer.

over a set time interval. We measured the breakup length in 158 separate experiments using either a high-speed camera (Phantom TMX 7510) or a regular camera with a fast flashlight (Vela One). We used simple image analysis (Python) to determine the jet lengths and the modulations of the jet thickness [Fig. 3(a)]. We excluded turbulent jets because the onset of turbulence quickly reduces the jet length [9]. Because the breakup length naturally fluctuates, we estimated it by averaging over a large number of measurements. Most of the experiments were conducted on an optical table, and no particular effort was made to isolate the experiment from external sources of noise such as the pumps or the fan of the high-speed camera.

To examine the origin of the initial disturbances, we first test the prevailing idea that nozzle imperfections and environmental noise cause the jet breakup by performing experiments using a variety of nozzles with different geometries (Fig. 2), wall roughnesses, and liquid flow profiles. Although the onset of turbulence is clearly influenced by nozzle quality, as long as the jet remains laminar it made no difference whether smooth, high-quality tapered nozzles, or capillaries with rough outlets were used. To study the effect of environmental noise [17,18], we minimized acoustic coupling with the environment by performing the experiments on an optical table in an isolated plexiglass chamber, using an external HPLC pump with a minimal noise level. The chamber was placed in vacuum to further minimize noise, and the pump was connected to the spray nozzle using a long and thin flexible plastic tube. Even at this level of isolation, we could not

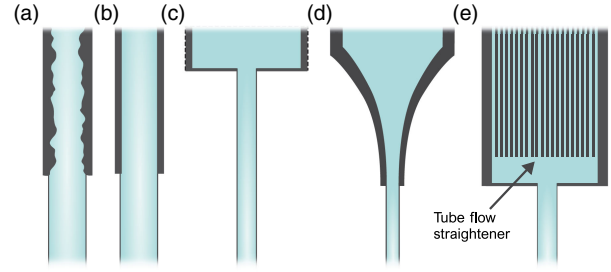


FIG. 2. Jet nozzle geometries. (a) Stainless steel needles with a flat end (Techcon) and relatively rough inner surfaces. (b) Glass capillaries, with very smooth inner surfaces. (c) Flat-plate nozzles, ranging from thin metallic plates with holes of uneven perimeter to microfabricated silicon spray nozzles (Medspray) with smooth holes. (d) Smooth stainless steel jet nozzles with tapered profiles (Schlick). (e) Jet orifices cut by electrical discharge machining in thin metallic plates attached to a flow straightener made using plastic straws, sponges, and meshes to suppress turbulence.

detect any increase in breakup length for several different liquid velocities. This suggests that background noise becomes unimportant below a certain threshold.

How initial disturbances affect breakup becomes most apparent when the jet surface is actively perturbed. Figure 1 shows perturbed (left) and unperturbed (right) jets issuing from a single nozzle with 64  $\mu\text{m}$  diameter [Fig. 1(a)], and from eight adjacent holes with 16  $\mu\text{m}$  diameter [Fig. 1(b)]. In both cases, an immersed piezoelectric transducer was used to generate controlled disturbances on the jet surface. The impact of controlled perturbations is profound: not only do the excitations result in perfectly monodisperse droplets, but the jet length is also significantly reduced.

The relationship between initial disturbances and jet breakup is described by Rayleigh's linearized perturbation theory [7]. Rayleigh showed that an axisymmetric jet is inherently unstable due to its out-of-equilibrium energy state, leading to the so-called Rayleigh-Plateau instability, in which small disturbances on the jet's surface grow exponentially. The radius  $R(z, t)$  of the jet varies as

$$R(z, t) = R + \delta_k \cos(kz) e^{\Omega_k t}, \quad (1)$$

where  $R$  is the initial radius of the jet,  $z$  the distance from the nozzle,  $t$  time, and  $k$  and  $\delta_k$  the wave number and amplitude of the perturbation, respectively. The growth rate  $\Omega_k$  is given by the dispersion relation [6–8],

$$\Omega_k = \sqrt{\frac{\gamma}{4\rho R^3} (\sqrt{2(x^2 - x^4) + 9Z^2 x^4 - 3Zx^2})}, \quad (2)$$

where  $x = kR$ , and  $Z = \mu/\sqrt{2\rho R\gamma}$  is the Ohnesorge number. The unstable modes have wavelengths larger than the jet's perimeter ( $|kR| < 1$ ), and the wavelength  $\lambda_R$  and frequency of the fastest growing mode are called the

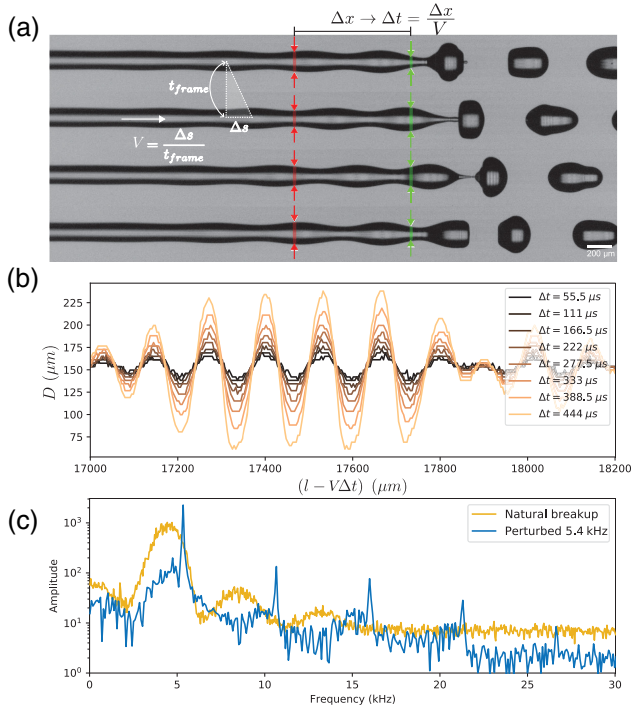


FIG. 3. Analysis of jet undulations with  $R = 75 \mu\text{m}$  and  $\Delta t = 55.5 \mu\text{s}$ . (a) Four consecutive images of an unperturbed water jet destabilizing. Using image analysis, the width of the jet is determined for a sequence of high-speed images at different positions, illustrated with red and green arrows. (b) Evolution of the spatially varying jet width  $D$ , corrected for the distance traveled. (c) Fourier analysis of the jet's surface for natural breakup (orange) and external perturbation at  $f = 5.4 \text{ kHz}$  (blue).

Rayleigh wavelength and frequency. Even the smallest axisymmetric disturbance on the jet's surface is strongly amplified, ultimately leading to breakup after a time  $T_k$  at which the perturbation's amplitude  $\delta_k e^{\Omega_k T_k}$  is of the order of  $R$ . At constant jetting speed  $V$ , we can therefore estimate the breakup length  $L_k$  of a perturbed jet to be

$$L_k = VT_k = \frac{V}{\Omega_k} \ln\left(\frac{R}{\delta_k}\right). \quad (3)$$

The jet length is therefore a direct measure of the amplitude of the initial disturbance for a perturbation with a fixed wavelength. The logarithmic dependence in Eq. (3) leads to a weak dependence of the breakup length on the perturbation level  $\delta_k$ , which may explain the difficulty in determining the origin of the perturbations. However, the change in breakup length becomes apparent if there are large differences in  $\delta_k$ , as there are between the unperturbed and perturbed jets in Fig. 1.

Figure 3(a) shows consecutive frames of a destabilizing jet. Using image analysis, the width of the jet can be determined at a given point in the lab frame for the whole duration of the video, resulting in a sinusoidal wave pattern.

By doing this for various distances from the nozzle, we can resolve the evolution of the disturbances. An example is shown in Fig. 3(b). A Fourier transform of this pattern shows higher harmonics appearing close to the breakup point [Fig. 3(c)]. These higher harmonics are probably due to the nonlinearity of the final phase of the droplet pinch-off when the deformed jet shape is no longer sinusoidal [19,20]. Within the resolution of our measurements, the wave pattern itself remains unchanged apart from its amplitude. This makes it unlikely that the pinch-off itself introduces perturbations that travel upstream [21], since these would be noticeable in this analysis. Instead, our analysis confirms Rayleigh's original idea that initial disturbances determine the jet length through (3). Only at very low velocities, near the dripping-to-jetting transition, is there a clear backpropagation of capillary waves, leading to a distinctly different breakup pattern, as demonstrated earlier by Umemura [22]. However, this represents a separate regime not addressed in this Letter.

A comparison of the Fourier spectra for perturbed and unperturbed jets reveals a clear difference. The spectrum of a perturbed jet exhibits a series of sharp, regularly spaced peaks, as expected from the applied sinusoidal forcing. In contrast, the spectrum of an unperturbed jet is smooth, broad, and centered around the Rayleigh frequency. This confirms the assumption leading to (3), and supports the idea of a random (or noisy) origin of the initial disturbances.

We consider two possible intrinsic sources of disturbances: the jet breakup itself or the intrinsic roughness of the liquid surface. Starting with the former, we note that the pinch-off of droplets—which “kick” the jet at around the resonant frequency—might be the main source of irremovable disturbances, which could travel back up to the nozzle and induce another breakup event after a time  $\Delta t \sim L_{\text{break}}/V$ . Savart already demonstrated that the breakup self-organizes to a steady mode when the impact of the stream of produced droplets is acoustically coupled to the nozzle [10,21]. As there is no such steady breakup for the unperturbed jet, it seems unlikely that the breakup length is self-limited. Still, to further test this idea, we studied a jet falling onto a liquid bath just above the breakup point. The bath was then quickly lowered while the jet length was recorded with a high-speed camera. On the timescale of the breakup, the lowering of the liquid bath is slow, as the jet speed  $\approx 10 \text{ m s}^{-1}$ . If the breakup itself is a source of perturbations, then increasing the distance between liquid bath and nozzle should temporarily extend the jet's length, or cause some oscillatory or transitory response due to the time needed for disturbances caused by the jet impact to travel upstream. However, we were unable to observe any increase or decrease of the jet length, even when actively perturbing the jet from below by placing an ultrasonic transducer in the liquid bath.

These results do not support a role for breakup-driven feedback. Instead, they point to intrinsic perturbations near the orifice as the cause of breakup in unperturbed jets.

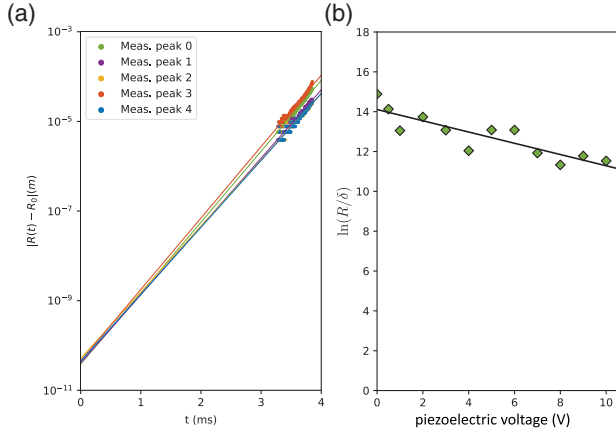


FIG. 4. Growing disturbances. (a) Exponential fits of tracked thickness modulations on the surface of the jet, as in Fig. 3. They intersect the  $y$  axis at  $\delta_0 \simeq 1 \text{ \AA}$ . (b) Logarithmic factors derived from the exponential fits of the growth of the perturbations for different voltage levels of the piezoelectric transducer.

Returning to Rayleigh’s theory, we use data such as those shown in Fig. 3(b), tracking the growth of disturbances on the jet surface and extrapolating the exponential growth back to  $t = 0$ , that is, the origin of the jet at the nozzle. This allows one to estimate the magnitude of the initial perturbations through (1). Figure 4(a) shows several examples of such exponential fits, all of which intersect with the  $y$  axis at  $\delta_0 \approx 1 \text{ \AA}$ . Although this method is imprecise, as there is a large range of length scales not covered by the experiments, it still provides a reasonable estimation of  $\delta_0$ . Moreover, earlier work [9] showed that the breakup length (3) for silicone oils reached a plateau at  $\ln(R/\delta) \approx 15$ , i.e.,  $\delta_0 \approx 1 \text{ \AA}$ . Though the authors did not address the origin of this plateau, the implied length scale is consistent with our proposed breakup model.

As an additional test that the breakup length is caused intrinsically, we study actively perturbed jets. If the disturbance leading to breakup is intrinsic, the jet length should reach its unperturbed length as the amplitude of the applied perturbation approaches zero. Conversely, one would anticipate a nonzero minimum amplitude for inducing breakup if the noise is of external origin. We applied a 5.4 kHz sinusoidal disturbance, using an immersed piezoelectric transducer. By increasing the amplitude of the perturbation, the jet length is continuously shortened, corresponding to a smaller logarithmic prefactor  $\ln(R/\delta)$  in (3). Figure 4(b) shows this prefactor as a function of the transducer voltage, where  $\delta$  is obtained through exponential fits as in Fig. 4(a). The jet length goes monotonically to its unperturbed length as the voltage decreases to zero, without a plateau, demonstrating that the active perturbation reaches the level of irremovable perturbations  $\delta_0$  at a near-zero voltage level. This means that  $\delta_0$  must be extremely small. In fact, our transducer changes  $\delta$  by a factor  $e^2 \simeq 8$  by increasing the amplitude; since the original

perturbation is at the  $\text{\AA}$  level, the perturbation imposed by the transducer is nanometric.

Assuming a noisy origin of the residual disturbance  $\delta_0$ , one would expect that on average the jet should break up at the frequency of the fastest growing mode, i.e., the Rayleigh frequency. The natural breakup length  $L$  thus corresponds to Eq. (3) calculated at the Rayleigh wavelength and with  $\delta_k = \delta_0$ . This yields the familiar scaling relation for the breakup length of an unperturbed jet [8,9], which we write in terms of the diameter  $D = 2R$ ,

$$\frac{L}{D} = \ln\left(\frac{D}{2\delta_0}\right) \text{We}^{1/2} (1 + 3Z), \quad (4)$$

where  $\text{We} = \rho DV^2/\gamma$  is the Weber number. Predicting the natural breakup length of a jet thus requires knowing  $\delta_0$ , as it sets the coefficient of Eqs. (3) and (4), i.e.,  $\ln(R/\delta) = \ln(D/2\delta)$ .

To estimate the initial perturbation we turn to capillary wave theory. Because the spectrum of thermal capillary waves corresponds to the Fourier transform of the thermally roughened surface, we can define  $\delta_0$  as the average effective amplitude of thermal capillary modes at the Rayleigh wavelength. A liquid cylinder of area  $A$  and temperature  $T$  has an effective capillary wave spectrum,

$$\delta_{\text{eff}}(k) = R \sqrt{\frac{k_B T}{\gamma A} \frac{1}{|(kR)^2 - 1|}}, \quad (5)$$

where  $k_B$  is the Boltzmann constant. Equation (5) can be derived using the equipartition theorem, and for stable modes ( $|kR| \geq 1$ ),  $\delta_{\text{eff}}$  represents the average amplitude of sinusoidal thermal perturbations at thermal equilibrium (the “static spectrum” [23]). Now the excess surface energy  $\delta E$  of an infinitesimally small sinusoidal perturbation on a cylinder of area  $A$  is given by  $\delta E = \gamma A(k^2 - 1/R^2)\delta_k^2/2$ , which equals  $k_B T/2$  at thermal equilibrium. Unstable modes that are amplified in time through (1) are not strictly speaking in hydrodynamic equilibrium, making (5) an effective spectrum with an associated average amplitude  $\delta_{\text{eff}}(k)$ .

The next step is to choose the appropriate value of the area  $A$ . The breakup process should be dominated by local perturbations, since Eq. (5) requires the smallest possible (local) area  $A_{\text{min}}$  to produce the largest possible perturbation. Capillary waves are normal modes that can only exist on the jet at a minimum length  $L_0$  of the order of the wavelength. This sets  $L_0 \simeq \lambda_R \simeq \sqrt{2\pi}D$  and  $A_{\text{min}} = \pi D L_0 \simeq \sqrt{2}\pi^2 D^2$ , which when introduced into (5) together with the resonance condition  $k = k_R$  yields

$$\delta_0 = \sqrt{\frac{k_B T}{\sqrt{8}\pi^2 \gamma}}. \quad (6)$$

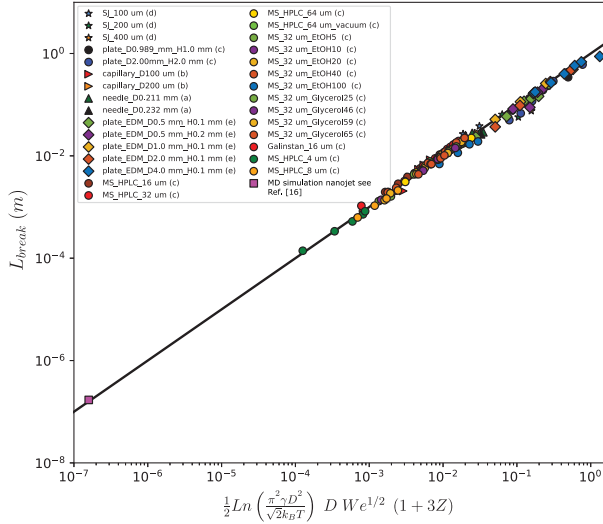


FIG. 5. Measured jet lengths  $L_{\text{break}}$  for various nozzle geometries, liquid velocities, fluid properties, and nozzle diameters versus the predicted value according to Eq. (7). The result from MD simulations of a nanojet is also included [16]; see bottom left of the figure.

For water ( $\gamma = 73 \text{ mN m}^{-1}$ ) at  $T \sim 300 \text{ K}$ , we find  $\delta_0 = 0.5 \text{ \AA}$ , which is consistent with our earlier observations. Note that this predicts a constant  $\delta_0$  for any jet size, which means that the prefactor  $\ln(R/\delta_0)$  of Eq. (3) and the scaling law (4) depend logarithmically on the radius  $R$ . Finally, substituting Eq. (6) into (4) gives the “unperturbed” jet breakup length:

$$\frac{L}{D} = \frac{1}{2} \ln \left( \frac{\pi^2 \gamma D^2}{\sqrt{2} k_B T} \right) \text{We}^{1/2} (1 + 3Z). \quad (7)$$

Figure 5 shows the breakup length calculated using Eq. (7) against the measured breakup length for various experimental conditions. The breakup length taken from MD simulations [16] of nanoscale jets is also included; see Fig. 3E in Ref. [16], where the results of MD simulations are shown to agree well with those obtained from a thermal hydrodynamic stochastic lubrication equation (SLE) treatment with the stochastic forces operative at all times, in contrast with the results of deterministic hydrodynamic lubrication equation (LE) calculations which were found to fail to predict both the jet’s breakup length and the profile of the pinch-off shape uncovered by the MD and SLE simulations. The prediction, which has no fitting parameters, yields a mean squared relative residual value of 0.04, whereas fitting for a constant logarithmic factor gives a value of 0.06.

Even though we propose a thermally driven model, the dependence on  $T$  is more difficult to probe: for water the accessible temperature range is too small to significantly change the logarithmic factor. For “cold” liquids such as liquid nitrogen, their much lower surface tension compensates for

the lower temperature in Eq. (7). Further studies could employ exotic jets at atypical temperatures, such as helium jets [24] or systems with ultralow interfacial tension [25]. Note that the Ohnesorge number is often very small and can be neglected, so that the Rayleigh wavelength can be approximated as  $\lambda_R = \pi D \sqrt{2(1 + 3Z)} \simeq \sqrt{2} \pi D$ .

In conclusion, we challenge the long-standing belief that external noise or nozzle imperfections are always the primary causes of laminar jet breakup. While strong external disturbances can affect the jet length, our findings show that under typical experimental conditions external influences become negligible. In the laminar regime, jet breakup lengths show no significant variation across diverse liquids and nozzle geometries, suggesting a breakup mechanism independent of nozzle quality or flow profile. In fact, intrinsic thermal capillary waves set an unavoidable background of effective disturbances at unstable Rayleigh-Plateau frequencies that can cause jet breakup. Our thermally induced breakup model predicts experimental observed jet breakup lengths over more than 7 orders of magnitude, from nanojets to macroscopic jets, without adjustable parameters. Using these insights, we can better predict and control jet behavior across a wide range of conditions.

*Acknowledgments*—This research has been funded by the Dutch Research Council NWO, IPP grant “Innovative Nanotech Sprays,” ENPPS.IPP.019.001, and supported by FCT—Fundação para a Ciência e Tecnologia, I.P. by Project No. 2023.02264.BD [Project DOI: 10.54499/2023.02264.BD]. N. M. R. was supported in part by the Horizon Europe ERC Grant No. 101098375\_SOFT-PLANET.

*Data availability*—The data that support the findings of this article are not publicly available. The data are available from the authors upon reasonable request.

- [1] D. Lohse, Fundamental fluid dynamics challenges in inkjet printing, *Annu. Rev. Fluid Mech.* **54**, 349 (2022).
- [2] M. X. Zhang, F. Verhoeven, P. Ravensbergen, S. Kooij, R. Geoffrion, D. Bonn, and C. J. van Rijn, Improved olfactory deposition of theophylline using a nanotech soft mist nozzle chip, *Pharmaceutics* **16**, 2 (2023).
- [3] D. D’Angelo, S. Kooij, F. Verhoeven, F. Sonvico, and C. van Rijn, Fluorescence-enabled evaluation of nasal tract deposition and coverage of pharmaceutical formulations in a silicone nasal cast using an innovative spray device, *J. Advert. Res.* **44**, 227 (2023).
- [4] A. Ziaee, A. B. Albadarin, L. Padrela, T. Femmer, E. O’Reilly, and G. Walker, Spray drying of pharmaceuticals and biopharmaceuticals: Critical parameters and experimental process optimization approaches, *Eur. J. Pharm. Sci.* **127**, 300 (2019).
- [5] A. Gharsallaoui, G. Roudaut, O. Chambin, A. Voilley, and R. Saurel, Applications of spray-drying in microencapsulation

- of food ingredients: An overview, *Food Res. Int.* **40**, 1107 (2007).
- [6] J. Eggers and E. Villermaux, Physics of liquid jets, *Rep. Prog. Phys.* **71**, 036601 (2008).
- [7] L. Rayleigh, On the capillary phenomena of jets, *Proc. R. Soc. London* **29**, 71 (1879).
- [8] C. Weber, Zum zerfall eines flüssigkeitsstrahles, *ZAMM-J. Appl. Math. Mech./Z. Angew. Math. Mech.* **11**, 136 (1931).
- [9] R. E. Phinney, Stability of a laminar viscous jet—the influence of the initial disturbance level, *AIChE J.* **18**, 432 (1972).
- [10] R. J. Donnelly and W. Glaberson, Experiments on the capillary instability of a liquid jet, *Proc. R. Soc. A* **290**, 547 (1966).
- [11] D. Rutland and G. Jameson, A non-linear effect in the capillary instability of liquid jets, *J. Fluid Mech.* **46**, 267 (1971).
- [12] T. A. Kowalewski, On the separation of droplets from a liquid jet, *Fluid Dyn. Res.* **17**, 121 (1996).
- [13] A. M. Gañán-Calvo, H. N. Chapman, M. Heymann, M. O. Wiedorn, J. Knoska, B. Gañán-Riesco, J. M. López-Herrera, F. Cruz-Mazo, M. A. Herrada, J. M. Montanero *et al.*, The natural breakup length of a steady capillary jet: Application to serial femtosecond crystallography, *Crystals* **11**, 990 (2021).
- [14] C. Zhao, D. A. Lockerby, and J. E. Sprittles, Dynamics of liquid nanothreads: Fluctuation-driven instability and rupture, *Phys. Rev. Fluids* **5**, 044201 (2020).
- [15] B. Barker, J. B. Bell, and A. L. Garcia, Fluctuating hydrodynamics and the Rayleigh–Plateau instability, *Proc. Natl. Acad. Sci. U.S.A.* **120**, e2306088120 (2023).
- [16] M. Moseler and U. Landman, Formation, stability, and breakup of nanojets, *Science* **289**, 1165 (2000).
- [17] F. Savart, Mémoire sur la constitution des veines liquides lancées par des orifices circulaires en mince paroi, *Ann. Chim. (Paris)* **53**, 337 (1833).
- [18] P. Lafrance and R. C. Ritter, Capillary breakup of a liquid jet with a random initial perturbation, *J. Appl. Mech.* **44**, 385 (1977).
- [19] M.-C. Yuen, Non-linear capillary instability of a liquid jet, *J. Fluid Mech.* **33**, 151 (1968).
- [20] D. F. Rutland and G. J. Jameson, A non-linear effect in the capillary instability of liquid jets, *J. Fluid Mech.* **46**, 267 (1971).
- [21] H. González, J. Arcenegui, F. J. García de Bollullos, J. R. Castrejón-Pita, and A. A. Castrejón-Pita, Self-stimulated capillary jet, *Phys. Rev. Appl.* **15**, 014054 (2021).
- [22] A. Umemura, Self-destabilizing mechanism of a laminar inviscid liquid jet issuing from a circular nozzle, *Phys. Rev. E* **83**, 046307 (2011).
- [23] Y. Zhang, J. Sprittles, and D. Lockerby, Thermal capillary wave growth and surface roughening of nanoscale liquid films, *J. Fluid Mech.* **915**, A135 (2021).
- [24] R. M. P. Tanyag, A. J. Feinberg, S. M. O. O’Connell, and A. F. Vilesov, Disintegration of diminutive liquid helium jets in vacuum, *J. Chem. Phys.* **152**, 234306 (2020).
- [25] Y. Hennequin, D. G. A. L. Aarts, J. H. van der Wiel, G. Wegdam, J. Eggers, H. N. Lekkerkerker, and D. Bonn, Drop formation by thermal fluctuations at an ultralow surface tension, *Phys. Rev. Lett.* **97**, 244502 (2006).